Elucidating cyclic AMP signaling in subcellular domains with optogenetic tools and fluorescent biosensors

Christina Klausen[1#], Fabian Kaiser[1#], Birthe Stüven[1#], Jan N. Hansen[1#], Dagmar Wachten[1,2*]

[1] Institute of Innate Immunity, Biophysical Imaging, University Hospital Bonn, University of Bonn, 53127 Bonn, Germany

[2] Research Group Molecular Physiology, Center of Advanced European Studies and Research (caesar), 53175 Bonn, Germany

# equally contributed

* corresponding author: Dagmar Wachten, Institute of Innate Immunity, Biophysical Imaging, University Hospital Bonn, University of Bonn, 53127 Bonn, Germany, dwachten@uni-bonn.de, +49-228-9656-311

Abstract

The second messenger 3´, 5´-cyclic nucleoside adenosine monophosphate (cAMP) plays a key role in signal transduction across prokaryotes and eukaryotes. Cyclic AMP signaling is compartmentalized into microdomains to fulfil specific functions. To define the function of cAMP within these microdomains, signaling needs to be analyzed with spatiotemporal precision. To this end, optogenetic approaches and genetically encoded fluorescent biosensors are particularly well suited. Synthesis and hydrolysis of cAMP can be directly manipulated by photoactivated adenylyl cyclases (PACs) and light-regulated phosphodiesterases (PDEs), respectively. In addition, many biosensors have been designed to spatially and temporarily resolve cAMP dynamics in the cell. This review provides an overview about optogenetic tools and biosensors to shed light on the subcellular organization of cAMP signaling.

Introduction

The second messenger 3´, 5´-cyclic AMP (cAMP) controls cellular signaling across all species. Cyclic AMP metabolism is controlled by adenylyl cyclases (ACs) and phosphodiesterases (PDEs) (1, 2). Transmembrane AC activity is regulated by G-protein coupled receptors (GPCRs) (3). Over the last decades, the concept of cAMP signaling evolved from a model where cAMP diffuses freely through the cytoplasm and slowly regulates metabolic processes (4) to the concept that cAMP uses compartmentalized signaling cascades to orchestrate various cellular and physiological functions (5).

To manipulate cAMP-dependent cellular signaling, pharmacology is widely used. However, this approach lacks spatial and temporal control. Hence, the application of optogenetics to manipulate and analyze cAMP signaling has gained increasing importance over the last years. Optogenetics is the combination of genetic and optical methods to achieve gain or loss of function in cells with minimal toxic effects (6). Besides optogenetic tools, biosensors have been developed that allow to study cAMP signaling with subcellular resolution.

Architecture of optogenetic tools

Optogenetic actuators consist of a modular architecture that includes a photosensor and an effector module (7). The photosensor module incorporates a chromophore, which absorbs a photon to undergo a photocycle. This cycle encompasses photochemical reactions within the chromophore, resulting in a light-adapted state (8), which is reversible in most photosensors. Structural changes within the chromophore are transduced to the effector module, regulating its activity (9). Photosensor modules are found across all species and can be grouped according to the chromophore and light-sensing protein modules (10). Flavin-binding photoreceptors react to blue light and include Light-Oxygen-Voltage (LOV) and Blue-Light using Flavin-Adenine Dinucleotide (BLUF) proteins. Rhodopsins incorporate retinal as a chromophore and respond to a wide spectral range (Fig. 1). The broadest spectral range is covered by the phytochromes, which bind a linear tetrapyrrole (bilin) as chromophore and include plant phytochromes (Phys), cyanobacteriochromes (CBCRs), and bacteriophytochromes (BphP).

Photoactivated adenylyl cyclases and phosphodiesterases

Most of the naturally occurring photoactivated ACs (PACs) are activated by blue light, e.g. the PACs found in *Beggiatoa sp.* (bPAC), *Eucena gracilis* (euPAC), *Oscillatoria acuminata* (OaPAC), *Naegleria gruberi* (NgPAC), or *Microcoleus chthonoplastes* (mPAC). These proteins rely on BLUF and LOV domains with a factor difference in activity between the dark and the light-adapted state (e.g. 100- to 300-fold for bPAC) (11, 12), but the activating blue light shows only poor tissue penetration and might evoke phototoxic effects. Additionally, these PACs cannot be actively inactivated, which is only a feature of the cyanobacteriochrome-based cPAC from *Microcoleus sp.* (13).

As of now, a naturally occurring red light-regulated PAC has not been discovered. Thus, several synthetic proteins have been designed, predominantly containing a bacteriophytochrome as photosensory domain. IlaC, the first synthetic red light-dependent AC, contains the photosensor module of the *Rhodobacter sphaeroides* bacteriophytochrome BphG1 fused to the adenylyl cyclase domain from *Nostoc sp.* CyaB1 (14). Another approach

combined the *Deinococcus radiodurans* photosensor module (*Dr*BphP) and the Cya2 effector module from *Synechocystis sp.* (15). Cya2 constitutes a guanylyl cyclase (GC), but can be converted into an AC by introducing a single point mutation (16). To improve the reversibility, the *Dr*BphP module was exchanged to the homologous bacteriophytochrome module from *Deinococcus deserti*, resulting in *Dd*PAC, which showed reversibility upon far red-light exposure (17). Similarly, CaRhGC, composed of rhodopsin fused to the GC from *Catenaria anguillulae,* and RhoGC from *Blastocladiella emersonii* were converted into a PAC by introducing two point mutations each (18, 19).

So far, only one naturally occurring PDE containing a photosensor module, the RhoPDE from *Salpingoeca rosetta,* has been identified (20, 21). The protein acts as a cGMP-selective phosphodiesterase, but the activity does not appear to be modulated by light. The protein is also active with cAMP as a substrate, but with a roughly 5-7-fold lower k_{cat} (22). The engineered red light-activated cAMP- and cGMP-specific PDE LAPD was generated similarly to PaaC by combining the *Dr*BphP with the effector module of *Homo sapiens* PDE2A (23). Table 1 summarizes the optogenetic tools that synthesize or hydrolyze cAMP.

Measuring cAMP dynamics using genetically encoded fluorescent biosensors

Direct and indirect fluorescent biosensors measure changes in cAMP levels or its downstream effects, respectively. The latter comprises only one family of fluorescent biosensors that report protein kinase A activity (24-27).

FRET-based biosensors

Direct cAMP biosensors include a cyclic nucleotide-binding domain (CNBD) of a cyclic-nucleotide effector protein fused to a single or more fluorophores. Most of these sensors are based on Förster Resonance Energy Transfer (FRET), where cAMP binding to the CNBD changes its conformation and, thereby, alters FRET between the donor and acceptor. FRET is inversely proportional to the sixth power of the distance between donor and acceptor fluorophore (28), whereby it provides a powerful method to measure incremental conformational changes induced by a change in cAMP levels.

Zaccolo *et al.* developed the first genetically encoded FRET-based cAMP biosensor by fusing the donor and acceptor of a FRET pair to the regulatory and catalytic subunit of protein kinase A (PKA), respectively (Figure 2A) (29). Despite the disadvantages that have been reviewed elsewhere (30), the activation kinetics and subcellular localizations reflect the response of native PKA, making this biosensor still usable for a number of applications (31). Over the years, several groups developed and improved single chain FRET sensors with different

characteristics regarding sensitivity, kinetics, and dynamic range (Figure 2B-C) (32-34). FRET-based biosensors are ratiometric, which allows calibrating the sensor, thereby normalizing for cell-to-cell variation in expression and inferring absolute cAMP concentrations from the FRET signal (35, 36).

Challenges in measuring cAMP using FRET-based biosensors

Measuring FRET requires correction for bleed-through and cross-excitation, often comprises a low signal-to-noise ratio, and the use of FRET sensors in fluorescent plate readers for high-throughput screenings (HTS) is difficult (37). In addition, most FRET sensors use donor/acceptor pairs near the blue light spectrum, as for combinations of green/red fluorescent proteins (FP) the FRET signal is too weak to be detected within the donor emission tail, whereby ratiometric imaging is impossible. This limits their application *in vivo* due to low tissue penetration of blue light and restricts the combination with blue-light based optogenetic tools to manipulate cAMP. In addition, the FP of the most common FRET pair, CFP and YFP, are vulnerable to pH changes and bleaching, and far-red/infrared FP have a low dynamic range due to a low quantum yield of far-red FP (38). Last but not least, fusion to subcellular-targeting domains can affect the sensor properties, which makes it difficult to directly compare cAMP signals of different subcellular locations (39).

Several approaches have tackled these problems and came up with solutions to improve existing sensors. These approaches used FP, improved for brightness, photostability, and pH-sensitivity (25, 40, 41), different sensor architecture to modulate the dynamic range and cAMP affinity (40-43), and novel topologies that allow universal targeting of the sensor without affecting its properties (39) (Figure 2). Of note, a cAMP biosensor for super-resolution imaging *in vivo* has been developed that is not based on FRET, but rather the proximity of one FP significantly alters fluorescence fluctuations of the other FP (FLINC-AKAR1, Figure 2D) (44).

Single-wavelength cAMP sensors

As an alternative to the FRET-based approach, single-wavelength cAMP sensors have been developed (Figure 2E-H), where, the CNBD is fused to only one fluorophore. Their design was inspired by single-fluorophore calcium indicators (GECIs). Here, the FP is engineered, whereby the pKa value and the orientation of the chromophore with respect to a fusion partner is altered, and an insertion of another protein, i.e. a CNBD, is tolerated. Upon ligand binding, the conformational change changes the fluorescence of the FP (45).

Without the second FP, however, single wavelength sensors are not ratiometric, i.e. they report rather qualitative than quantitative changes in cAMP levels. To ratiomerize a single-wavelength

cAMP biosensor, a second FP was fused at the C-terminus of the circularly permuted GFP (cpGFP) (Figure 2F) (46).

Nevertheless, the current diversity of single-wavelength cAMP sensors is still limited compared to FRET-based biosensors regarding sensitivity, dynamic range, and kinetics. Furthermore, red-shifted single-wavelength cAMP sensors are still inferior to currently used blue, yellow, and green FPs in terms of brightness, limiting their application for imaging of subcellular compartments (47).

Overall, the selection of a cAMP sensor for a given application can be challenging, depending on the scientific question and the available equipment. The list of sensors aims to help deciding for a state-of-the-art sensor (Table 2, 3). To apply these sensors in a given experiment, detailed descriptions for setting up, measuring, and evaluating fluorescent cAMP biosensors were described elsewhere (35, 38, 48).

AC and PDE activity assays

Besides using a biosensor, cellular cAMP dynamics can be measured by combining the expression of a cyclic nucleotide-gated (CNG) ion channel with fluorescent Ca^{2+} imaging. Here, a mutant CNG channel, which binds cAMP with higher affinity (CNGA2-TM), reports changes in the intracellular cAMP concentration with a concomitant Ca^{2+} influx that is detected using fluorescent Ca^{2+} dyes (49). This approach has been used to monitor endogenous and heterologously expressed AC (49) and PDE activity (50-53), and allows to test the activity of optogenetic cAMP-manipulating tools in a cellular assay (Figure 3).

Analyzing cAMP signaling in microdomains

Cyclic AMP signaling is compartmentalized into microdomains (54-56). Thus, analyzing and manipulating cAMP signaling requires a spatial precision that allows differentiating between subcellular compartments. Common targeting approaches rely on fusing optogenetic tools or biosensors to a targeting sequence or on a protein that localizes to a given microdomain. However, protein fusion might impair the functionality of optogenetic tools and biosensors. Therefore, designing a strategy for subcellular targeting of optogenetic tools is particularly challenging. In the following, we highlight innovative approaches to functionally localize optogenetic tools to different subcellular compartments. A detailed description of the targeting methods is summarized in Table 4.

Plasma membrane

Targeting to the plasma membrane has been achieved by fusion to common plasma membrane trafficking signals, such as peptide sequences that undergo lipid modifications.

However, the lipid content of the plasma membrane is compartmentalized into patches of defined lipid composition, i.e. lipid rafts (57). Targeting an Epac2-based FRET sensor to lipid rafts by fusion to a C-terminal isoprenylated CAAX box, and to non-lipid-raft regions by fusion to an N-terminal myristoylated and palmitoylated peptide sequence has unraveled two different identities of cAMP signaling at the plasma membrane: lipid-raft- and non-lipid-raft-associated cAMP signaling (58).

Cyclic AMP microdomains are defined by the presence of distinct scaffolding proteins (AKAPs), which can also be used for targeting. For example, the FRET-based sensor CUTie was fused to AKAP79 to target the sensor to a PKA-associated signalosome at the plasma membrane (39, 59). This approach unraveled that the basal cAMP concentration in a PKA-associated signalosome is not different from bulk cAMP levels in the cell, which had been previously proposed based on computational studies (60).

Ion channels in the plasma membrane control the membrane potential. Widely used optogenetic tools that control the membrane potential, i.e. channelrhodopsins, lack specificity and promiscuously conduct cations. Only in recent years, light-controlled ion channels with different ion selectivity have been generated. These tools have been created by combining optogenetic cAMP manipulation with the gating of potassium or calcium channels, i.e. fusion of PACs with the CNG channel mutant T537 (61) or SthK from *Spirochaeta thermophile* (61, 62).

Nucleus

Nuclear cAMP signaling is particularly important for cAMP-dependent, CREB (cAMP responsive element-binding protein)-controlled gene expression (63). To characterize the dynamics of nuclear cAMP signaling, in particular cAMP-dependent PKA activation, the nuclear import machinery has been hijacked by fusing a nuclear localization signal (NLS) to the C-terminus of Epac1-based cAMP-sensor ICUE1 (64) and the PKA-activity sensor AKAR4 (A-kinase activity reporter) (65). This revealed that the nuclear PKA response after cAMP production at the plasma membrane is largely delayed.

Mitochondria

Cyclic AMP signaling controls mitochondrial function, such as fusion, fission, and biogenesis (66). Many studies demonstrated the localization of PKA to specific sub-mitochondrial domains, mediated by distinct AKAPs (5). In an initial attempt to shed light on mitochondrial cAMP signaling, ICUE1 was targeted to the outer mitochondrial membrane or the mitochondrial matrix by fusion to targeting sequences adopted from the AKAP dAKAP1 or from the subunit IV of human cytochrome C oxidase, respectively (64). These experiments revealed

that cAMP in the mitochondrial matrix originates from cytoplasmic cAMP that is imported by an unknown mechanism (64). Later, this concept was challenged by functional studies on mitochondrial cAMP signaling, demonstrating that the inner mitochondrial membrane is impermeable for cAMP and that a resident AC in the outer mitochondrial matrix locally produces cAMP (67-69). Furthermore, scrutinizing the targeting described for ICUE1 (64) revealed that the construct is largely misplaced to the cytosol (70). However, fusing four copies of this targeting sequence (4mt) from subunit VIII of the human cytochrome oxidase to the EPAC-based sensor H30 (71) allowed to precisely localize the protein to the mitochondrial matrix and confirmed that cytosolic cAMP surges do not enter the mitochondrial matrix (70).

In the past years, mitochondrial cAMP-signaling domains have been further characterized using Epac-S^{H187} and EpacH90, as well as the PKA-activity sensors AKAR3 and AKAR4 that were targeted to the mitochondrial matrix using the 4mt targeting sequence or to the outer mitochondrial membrane by adopting from the mitochondrial import receptor subunit TOM70 (72, 73). AKAR3 was previously targeted to the outer mitochondrial membrane using the dAKAP1 (24).

Endoplasmic Reticulum (ER)

ER-translocation signals need to be fused at the N-terminus of a protein. Here, 18 amino acids of the signal sequence from BiP (binding protein, member of the hsp70 family) together with a modified KDEL sequence (AKDEL) are sufficient to retain proteins in the ER (74). This fusion approach has been applied to target a luciferase-coupled bPAC to the ER (bPAC-nLuc) (74). The nLuc luciferase uses its substrate coelenterazine-*h* (hCTZ) to emit blue-shifted luminescence that activates bPAC, whereby a long-lasting stimulation of bPAC activity is achieved that is not toxic to the cell. This approach can be coupled to short light-pulse activations to directly activate bPAC and has also been used for targeting to other subcellular domains, e.g. the plasma membrane, soma, and nucleus, revealing that cAMP synthesis in the cytosol and nucleus and not at the endoplasmic-reticulum stimulates cell proliferation in thyroid cells (74).

Cell-specific compartments

Neurons

Optogenetics has revolutionized the neurosciences. Targeting of optogenetic tools to specific neuronal compartments, e.g. synapses, has been applied for many optogenetic tools other than those controlling cAMP signaling. A comprehensive overview about this topic is provided elsewhere (75).

Cardiomyocytes

In cardiomyocytes, a unique compartment – the sarcoplasmic reticulum (SR) – contains cAMP signaling compartments. The SR represents the main Ca^{2+} storage in cardiomyocytes. Ca^{2+} uptake into the SR relies on SR Ca^{2+}-ATPases (SERCAs) that are regulated by cAMP/PKA-dependent phosphorylation of the SERCA-associated protein phospholamban, whereas Ca^{2+} release relies on ryanodine receptor (RyR) opening. FRET-based biosensors have been used to characterize different cAMP signaling microdomains in cardiomyocytes (76). For example, Epac1-camps has been targeted to the SERCA2a microdomain by fusion to the N-terminus of phospholamban (Epac1-PLN) (77), to the sodium-potassium ATPase in the cardiomyocyte plasmamembrane by fusion to the C-terminus of phospholemman (PLM-Epac1) (78), and to caveolin-rich sarcolemmal microdomains by N-terminally fusing a 10 amino-acid sequence of Lyn kinase (pmEpac1) (79). The latter Lyn-kinase-based targeting sequence was also successfully used for functional targeting of Epac2-camps (80). To study PKA activity in the SERCA microdomain, SR-AKAR3 was developed by fusion of AKAR3 to the helical transmembrane domain of phospholamban (81). For characterizing cAMP dynamics in the vicinity of RyR2, the targeted cAMP sensor Epac1-JNC was developed by fusion of Epac1-camps to the cytoplasmic N-terminus of junctin (JNC), which is in a complex with RyR2 (82).

Cilia and flagella

Cilia are membrane protrusions emanating from the cell surface and come in two different flavors: motile cilia/flagella are only found on specialized cells, where they control cell movement or the generation of fluid flow, whereas immotile primary cilia protrude from the surface of almost every mammalian cell. Cyclic AMP signaling controls the function of both, primary cilia and flagella, in particular sperm flagella (83, 84). The signaling cascades are, however, still not completely understood. Currently, only optogenetics and fluorescent biosensors allow sufficient spatio-temporal resolution to further characterize these pathways and, thus, have gained attention in cilia research. Optogenetics and fluorescent biosensors have first been applied in sperm flagella to study sperm motility and fertilization (50, 51, 85). Recently, those techniques have also been used to analyze cAMP signaling in primary cilia (46, 86, 87).

Optogenetic control of protein localization

Recently, the CIB1-CRY2 system has been applied to control the cellular localization of PKA by light. This revealed the role of PKA in different signaling domains (88). Here, CIB1 was fused to the targeting sequence, whereas CRY2 was fused to the C-subunit of PKA. In the dark, CIB1 and CRY2 do not interact. Upon light stimulation, a conformational change causes

their dimerization and thereby, targeting of PKA to a specific domain, i.e. the plasma membrane and the outer mitochondria membrane (88).

Perspective

The sensitivity and applicability of cAMP-specific optogenetic tools has been continuously improved, giving rise to many different ACs and PDEs. Similarly, cAMP biosensors are continuously evolving, providing diverse sensors with different spectral properties and sensitivity ranges. The diversity of optogenetic actuators and sensors offers the flexibility of choosing among different tools for optimizing a particular experimental setup. In addition, due to their wide spectral range, it is now possible to combine different cAMP-manipulating and -measuring tools in one assay. Applying these tools to subcellular compartments will lead to a more precise understanding of the manifold cellular functions of cAMP and open up new avenues in understanding cAMP signaling.

Conflict of interest

The authors declare no conflict of interest.

Acknowledgement and funding information

The project was supported by grants from the Deutsche Forschungsgemeinschaft (DFG): SPP1926: grant WA3382/2-1 (to DW), SPP1726: grant WA3382/3-1 (to DW), under Germany's Excellence Strategy – EXC2151 – 390873048 (to DW), and the Boehringer Ingelheim Fonds (to JNH).

Author contribution

All authors wrote and corrected the manuscript.

Abbreviations

AC	adenylyl cyclase
AKAP	A-kinase anchoring protein
AKAR	A-kinase activity reporter
Arl13B	ADP-ribosylation factor-like GTPase 13B
α-MHC	α-myosin heavy chain
BiP	binding immunoglobulin protein
BLUF	Blue-Light using Flavin-Adenine Dinucleotide
bPAC	photoactivated AC from *Beggiatoa* sp.
BphP	bacteriophytochromes
cAMP	3´, 5´-cyclic adenosine monophosphate
cAMPr	single-wavelength cAMP sensor
camps	cAMP sensor
CaRhGC	rhodopsin fused to the GC from *Catenaria anguillulae*
CBCR	cyanobacteriochrome
CD8	cluster of differentiation 8
cGMP	3´, 5´-cyclic guanosine monophosphate
CMV	cytomegalovirus promoter
CNBD	cyclic nucleotide-binding domain
CNG	cyclic nucleotide-gated
CNGA2-TM	cyclic nucleotide-gated ion channel A2 (TM mutant)
COX	cytochrome C oxidase
cp	circular permuted
cPAC	cyanobacteriochrome-based PAC from *Microcoleus sp.*
cpFP	circularly permuted fluorescent protein
cpmApple	circularly permuted mApple
cp173Venus	circularly permuted form of the Venus yellow fluorescent protein
CREB	cAMP response element-binding protein
CUTie	cAMP Universal Tag for imaging experiments
DAKAP1	*dual-specificity A-kinase anchoring protein 1*
*Dd*PAC	photoactivated AC from *Deinococcus deserti*
*Dr*BphP	*Deinococcus radiodurans* photosensor module
Dronpa	photoswitchable fluorescent protein
EC50	half-maximal effective concentration

Epac1	exchange protein directly activated by cAMP
euPAC	photoactivated AC from *Eucena gracilis*
Flamindo	fluorescent cAMP indicator
FLINC	fluorescence fluctuation increase by contact
FP	fluorescent protein
FRET	Förster Resonance Energy Transfer
GC	guanylyl cyclase
GECI	single-fluorophore calcium indicator
GPCR	G-protein coupled receptor
HCN2	cyclic nucleotide-gated potassium channel 2
hCTZ	coelenterazine-*h*
HTS	High-Throughput-Screening
ICUE	indicator of cAMP using Epac
JNC	junctin
K_D	equilibrium dissociation constant
LOV	Light-Oxygen-Voltage
Lyn	a tyrosine-protein kinase encoded by the LYN gene
Mito	mitochondrial targeting signal
MlotiK1	MlotiK1 potassium channel from the bacterium Mesorhizobium loti
mPAC	photoactivated AC from *Microcoleus chthonoplastes*
MYR	plasma-membrane-localization tag (amino acids 1-17 of the Yes protein)
MyrPalm	protein sequence that undergoes myristoylation and palmitoylation
n.a.	not available
NgPAC	photoactivated ACs from *Naegleria gruberi*
NLS	nuclear localization signal
nLuc	nanoLuc® luciferase
OLF	CNG channel mutant T537S
OMM	outer mitochondrial membrane tag adopted from TOM70
PAC	photoactivated AC
PDE	phosphodiesterase
Phy	plant phytochrome
PLM	phospholamban
PLN	phospholemman
PM or pm	plasma membrane

PKA	protein kinase A
Prm1	protamine 1 promotor
P2A	2A ribosome skip peptide from porcine teschovirus-1
R-FlincA	Red Fluorescent indicator for cAMP
RyR	ryanodine receptor
SR	sarcoplasmic reticulum
SthK	small cyclic nucleotide-gated potassium channel SthK
SERCA	SR Ca^{2+}-ATPase
SSTR3	Somatostatin receptor 3
tmAC	transmembrane adenylyl cyclase
TOM70 receptor subunit)	translocase of outer mitochondrial membrane 70 (mitochondrial import
T2A	2A ribosome skip peptide from thosea asigna virus 2A
YFP	yellow fluorescent protein
4mt	Repetitive (four copies) targeting sequences from subunit VIII of the human COX (tag also referred as 4Cox8 in other publications)
5-HT6	5-hydroxytryptamine-6-receptor
Z´	statistical measure to judge the assay quality

Figures

Figure 1

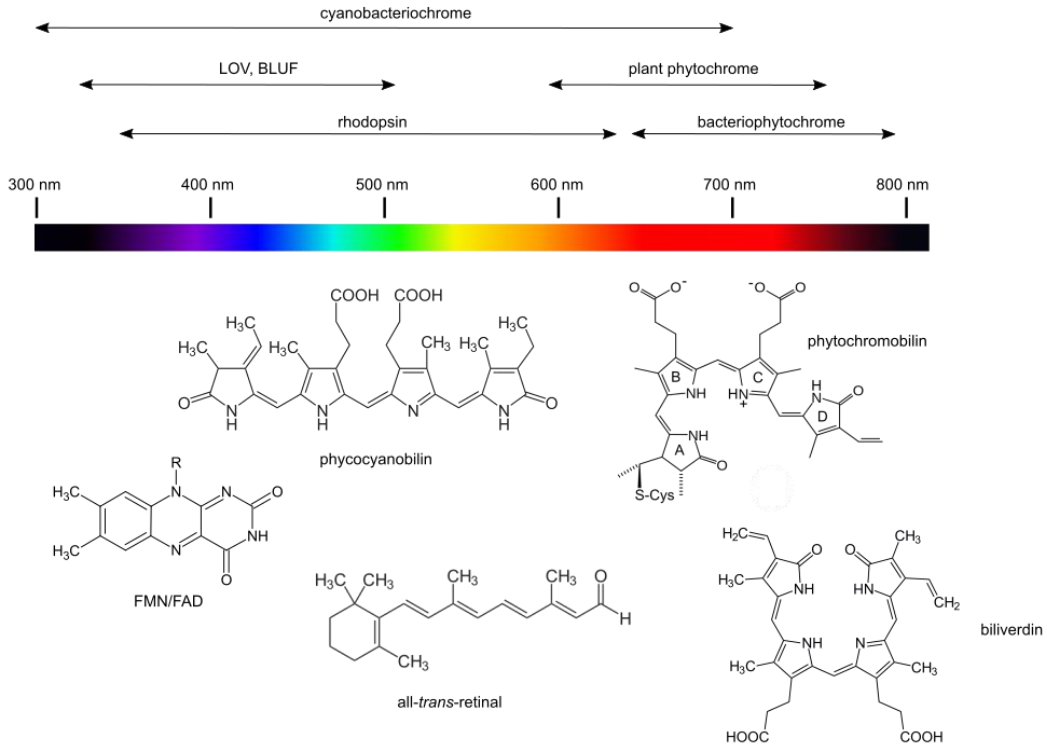

Figure 2

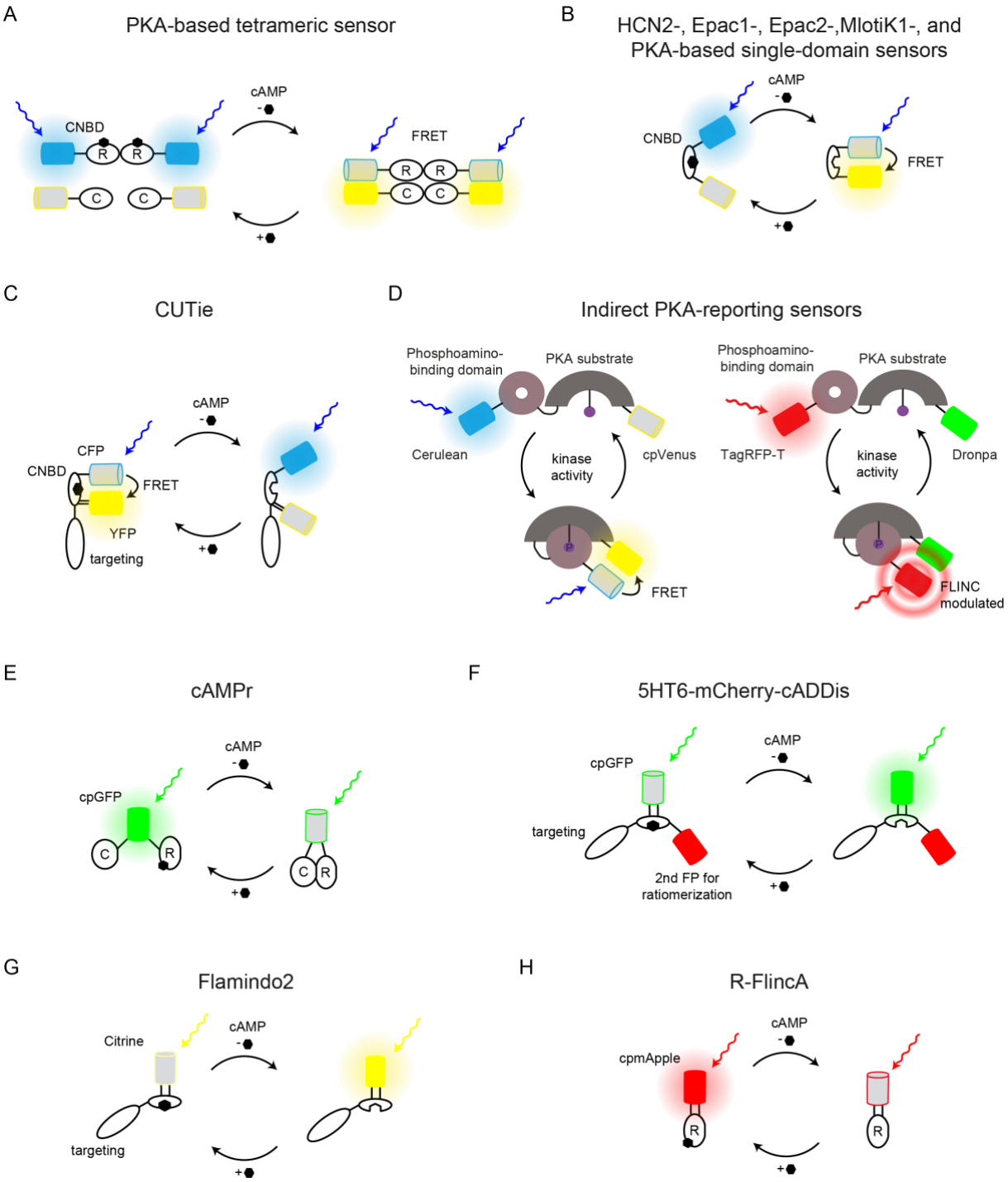
A
PKA-based tetrameric sensor
CNBD
R
R
C
C
cAMP
-
+
FRET
B
HCN2-, Epac1-, Epac2-,MlotiK1-, and
PKA-based single-domain sensors
CNBD
cAMP
-
+
FRET
C
CUTie
CFP
CNBD
FRET
YFP
targeting
cAMP
-
+
D
Indirect PKA-reporting sensors
Phosphoamino-
binding domain
PKA substrate
Cerulean
kinase
activity
cpVenus
FRET
Phosphoamino-
binding domain
PKA substrate
TagRFP-T
kinase
activity
Dronpa
FLINC
modulated
E
cAMPr
cpGFP
C
R
cAMP
-
+
F
5HT6-mCherry-cADDis
cpGFP
targeting
2nd FP for
ratiomerization
cAMP
-
+
G
Flamindo2
Citrine
targeting
cAMP
-
+
H
R-FlincA
cpmApple
R
cAMP
-
+

Figure 3

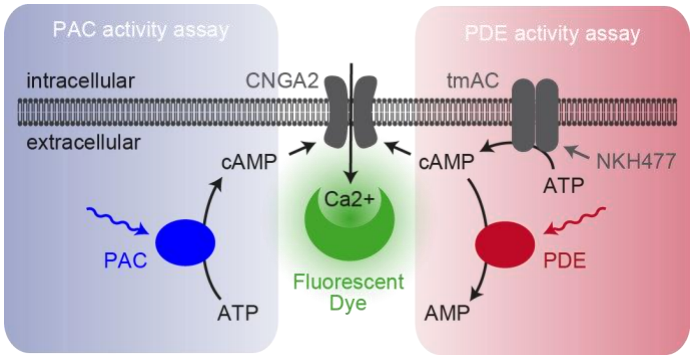
PAC activity assay
PDE activity assay
intracellular
extracellular
CNGA2
tmAC
cAMP
cAMP
NKH477
ATP
Ca2+
PAC
PDE
Fluorescent
Dye
ATP
AMP

Figure legends

Figure 1: Spectral range of photosensor modules found in photoactivated adenylyl cyclases (PACs) and light-regulated phosphodiesterases. The photosensors incorporate different chromophores to pass through a photocycle and allow photoswitchability, as indicated below the color spectrum. Adapted from (10).

Figure 2: Schematic overview of currently available fluorescent cAMP sensors. (A-D): FRET-based cAMP sensors. Binding of cAMP to the CNBD modulates the FRET signal of these sensors. An exception is the PKA-reporting sensor FLINC (fluorescence fluctuation increase by contact)-AKAR1(A-kinase activity reporter 1) depicted on the right (D), where the proximity of Dronpa modulates fluorescence fluctuations of TagRFP-T (S158T). (E-H): Single-wavelength cAMP sensors: Binding of cAMP to the CNBD modulates fluorescence of the chromophore. (G) To ratiomerize these sensors, another FP can be fused to the sensor (F).

Figure 3: Cellular assays to measure photoactivated adenylyl cyclase (PAC) or light-regulated phosphodiesterase (PDE) activity using a reporter HEK293 cell line expressing the cAMP-gated cation channel CNGA2 (49), which conducts Ca^{2+}. Here, changes in cAMP levels are indirectly reported through changes in Ca^{2+} levels reported using fluorescent Ca^{2+} dyes. Light-dependent activation of PACs increases intracellular cAMP levels, leading to a Ca^{2+} influx and, in turn, increased dye fluorescence. To measure PDE activity, cells are pre-stimulated with NKH477 to activate endogenous transmembrane adenylyl cyclases (tmAC). Activation of PDE by light decreases cAMP levels, and in turn Ca^{2+} levels.

Tables

Table 1: Overview of photoactivated adenylyl cyclases (PACs) and phosphodiesterases (PDEs). PACs and PDEs are either of natural or synthetic origin. Annotations in the table: *, main peak of activation/inactivation; +, full reversibility; ~, moderate reversibility; n.a., not available. Other abbreviations, see abbreviation list.

	origin	tool	Photosensory domain	Activation*	Inactivation*	Efficiency of inactivation	original literature
Adenylyl cyclases	Naturally occurring	cPAC	CBCR	410 nm	520 nm	+	(13)
		bPAC, OaPac, euPAC, NgPAC1-3	BLUF	450 nm	Dark reversion	+	(11) (bPAC), (89) (OaPAC), (90) (euPAC), (91) (NgPAC1), (92) (NgPAC2), (93) (NgPAC3)
		mPAC	LOV	450 nm	Dark reversion	+	(94)
	Synthetic	CaRhAC (naturally occurring as CaRhGC), RhGC (as AC)	Rhodopsin	530 nm	Dark reversion	n.a. CaRhAC, + RhoGC as AC	(18) (CaRhAC), (19) (RhoGC as AC)
		IlaC	BphP	650 nm	850 nm	n.a.	(14)
		PaaC, *Dd*PAC	BphP	650 nm	850 nm	~ PaaC + *Dd*PAC	(15) (PaaC), (17) (*Dd*PAC)
PDEs	Naturally occurring	RhoPDE	Rhodopsin	490 nm	Dark reversion	+	(21)
	Synthetic	LAPD	BphP	650 nm	750 nm	~	(23)

Table *2*: Overview of FRET-based cAMP sensors. List of abbreviations: AKAR, A-kinase activity reporter; CNBD, cyclic nucleotide-binding domain; CUTie, cAMP Universal Tag for imaging experiments; cp173Venus, Circularly permuted form of the Venus yellow fluorescent protein; ICUE3, Indicator of cAMP using Epac; HCN2, cyclic nucleotide-gated potassium channel 2; n.a., not available; K_D, equilibrium dissociation constant; EC50, Half maximal effective concentration to cAMP or cGMP; cGMP, Cyclic guanosine monophosphate. Other abbreviations, see abbreviation list.

Sensor	Sensitivity (k_D/ EC_{50})		Comment	Reference	Reference for initial construct
	cAMP	cGMP			
FLINC-AKAR1, Dronpa/TagRFP-T flank a phosphor-amino acid binding-domain (PAABD) fused to a PKA-specific substrate	n.a.	n.a.	**Indirect** sensor that is compatible with super-resolution imaging in live cells. Not FRET-based, but contains two fluorophores. "Flickering" of TagRFP-T is modulated by Dronpa proximity, which changes upon PKA-dependent phosphorylation of the PAABD	(44)	AKAR2 (26)
CUTie, YFP was inserted into a CNBD of PKA RIIβ and CFP fused to the CNBD C-terminus	EC_{50} = 7.4 µM	n.a.	New topology allows N-terminal targeting without altering sensor properties. Revealed differential cAMP kinetics and amplitudes of localized cAMP signals at distinct plasmalemma, sarcosplasmic reticulum, and myofilament sites.	(39)	Original construct
mlCNBD-FRET, CNBD domain of bacterial *Mloti*K1 channel sandwiched between Cerulean and Citrine	K_D 66 ± 15 nM	K_D 504 ± 137 nM	Highest affinity for all cAMP sensors. Used *in-vivo* to unravel sub-compartmental cAMP dynamics in the sperm flagellum. Fast kinetics and developed from a bacterial CNBD.	(85)	Original construct
PKA RIα #7, RIα, cAMP binding site of human PKA sandwiched between cp173Venus and ECFP	K_D 37.2 nM	n.a.	High sensitivity and dynamic range, allowed first measurement of extracellular cAMP acting as a chemo-attractant.	(43)	Original construct
Epac-S^{H188} / Epac-S^{H187} Epac2 CNBD-domain sandwiched between mTurquoise2 and tandem cpVenus	K_D 9.5 µM / 4 µM	n.a.	Less pH sensitive, enhanced photostability, dynamic range, and signal-to-noise ratio.	(41)	Epac-$S^{H21, H27, H30}$ (71)*
Epac-S^{H159} / Epac-S^{H189}, Epac2 CNBD-domain sandwiched between mTurquoise2 and a dark-acceptor	K_D 9.5 µM / 4 µM	n.a.	Designed for better performance in FLIM measurements.		
AKAR4, Cerulean/cpVenus flank a phosphor-amino acid binding-domain	EC_{50} 2.1 µM	n.a.	**Indirect sensor**, targeted with a myrstoylation/ palmitoylation sequence to membrane rafts and to non-rafts by a farnesylation lipid sequence. Visualized PLA activity in plasma membrane microdomains.	(25)	AKAR1 (27)

(PAABD) fused to a PKA-specific substrate					
ICUE3, Epac1 CNBD sandwiched between eCFP and cpVenus	Not tested, EC_{50} of ICUE2 12.5 ± 2.8 µM	n.a.	Myristoylation/palmitoylation for membrane targeting. Improved spatio-temporal resolution and dynamic range allowed to study the role of membrane microdomains in regulating ß-adrenergic-mediated cAMP dynamics in HEK293 cells.	(40)	ICUE (64)
Epac2-camp300, Epac2 CNBD sandwiched between CFP and YFP	EC_{50} 300 nM	EC_{50} 14.± 4 µM	Higher cAMP affinity than Epac2-camps. Allowed to measure and quantify low concentrations of cAMP in living follicle-enclosed mouse oocytes.	(42)	Epac2-camps (55)
HCN2-camps, CNBD domain of HCN2 channel sandwiched between EYFP and ECFP	EC_{50} 5.9 ± 0.3 µM	31.5 ± 2.3% of the cAMP signal at 600 µM	Fast kinetics and high dynamic range. Revealed differences in cardiac myocyte cAMP signaling of β_1- and β_2-adrenergic receptors.	(95)	Original construct
Epac1/2 camps, CNBD domains of Epac1 or Epac2 sandwiched between CFP and YFP	EC_{50} 2.4 / 0.9 µM	n.a.	Epac-based single chain architecture with fast kinetics.	(55)	Original construct
PKA-camps, PKA regulatory subunit RIIß sandwiched between CFP and YFP	1.9 µM	n.a.	PKA-based single chain architecture, no catalytic activity.	(55)	Original construct
C6H9 PKA, R- and C-subunit of PKA fused to CFP and YFP, respectively.	EC_{50} 5.2 µM cAMP	n.a. (same as endogenous PKA)	Tetrameric, reflects PKA kinetics to cAMP, remaining PKA activity.	(31)	Original construct

**Note that the Kees Jalink group updated the nomenclature of their sensors with introduction of the fourth-generation Epac-based FRET sensors for cAMP (41).*

Table 3: Overview about single wavelength cAMP sensors. cAMPr, Single wavelength cAMP sensor; R-FlincA, Red Fluorescent indicator for cAMP; cpmApple, circular permuted mApple; 5-HT6, 5-hydroxytryptamine-6-receptor; Flamindo2, fluorescent cAMP indicator 2; HTS, High-Throughput-Screening; Z´, statistical measure to judge the assay quality; NLS, nuclear localization signal; n.a., not available. Other abbreviations, see abbreviation list.

Sensor	Sensitivity (k_D/ EC_{50})		Comment	Reference	Reference for initial construct
	cAMP	cGMP			
cAMPr, cpGFP fused to PKA-C and PKA-R_{91-244}	K_D 1 µM	No response to 1mM cGMP	Established *in vivo* in drosophila brain, compatible with single- and two-photon imaging, linear response to cAMP	(96)	Original construct
R-FlincA, cpmApple sandwiched between two halves of PKA RIα subunit	K_D 0.3 µM	K_D 6.6 µM	Red cAMP biosensor. High affinity and increased dynamic range. High sensitivity allowed to measure small cAMP changes associated with spontaneous cellular signaling.	(47)	Pink-Flamindo (97)
5-mCherry-cADDis, cpGFP in between the catalityc and enzymatic domains of Epac2	K_D 10-100 µM	n.a.	Fused to a targeting protein at the N-terminus and a FP at the C-terminus to allow ratiometric cAMP measurements in the primary cilium. Only commercially available in BacMam system. Low affinity. Applied to measure Hedgehog signaling in the primary cilium. Initial construct was optimized for HTS (Z´of >0.75).	(46)	cADDis (98)
Flamindo2, mEpac1 CNBD sandwiched between two halves of Citrine	K_D 2.1 µM	K_D 22 µM	Yellow fluorescent cAMP indicator allowed dual-colour imaging with red fluorescent Ca^{2+} indicator and reported that forskolin elevated cAMP levels of the cytosol and nucleus of COS7 cells with different kinetics. Sensor remains functional after NLS fusion (N-terminal).	(99)	Flamindo (100)

Table 4: Overview about targeting approaches for optogenetic tools and fluorescent biosensors to manipulate and measure cAMP signaling, respectively; n.a., not available. Other abbreviations, see abbreviation list.

Tool	Targeted to	Targeting via	Promoter	Reference
Epac2-CAAX	Plasma membrane	CAAX box sequence (KKKKSKTKCVIM) from Rho GTPase fused to the C-terminus	CMV	(58)
Epac2-MyrPalm	Plasma membrane	Acylation sequence (GCINSKRKD) from Lyn kinase fused to the N-terminus		
AKAP79-CUTie	Plasma membrane	AKAP79 fused to the N-terminus	n.a.	(39, 59)
SthK-YFP-bPAC	Plasma membrane	SthK fused to the N-terminus	Oocytes: mRNA microinjection	(61)
Olf-bPAC	Plasma membrane	CNG (*Bos taurus* CNGA2) channel mutant T537S fused to the N-Terminus	*Drosophila melanogaster*: UAS	
CD8-YFP-bPAC	Plasma membrane	CD8 fused to the N-Terminus	*Drosophila melanogaster*: UAS	
SthK-P2A-bPAC(wt)-mCherry	Plasma membrane	SthK channel separated from the PAC by a 2A ribosome skip peptide from porcine teschovirus-1 (P2A)	Cardiomyocytes: CMV Neuronal expression: CaMKIIα	(62)
bPAC(S27A)-SthK-T2A-mCherry	Plasma membrane	SthK fused to the C-terminus by a peptide sequence (PRTYETSQVAPAGAP)		
Pm ICUE-1	Plasma membrane	KKKKKSKTKCVIM inserted at the C-terminus	CMV	(64)
NLS-ICUE-1	Nucleus	NLS sequence PKKKRKVEDA fused to the C terminus		
Mito-DAKAP1-ICUE1	Mitochondria	MAIQLRSLFPLALPGMLALLGWWWFFSRKK of DAKAP1a inserted at the N-terminus		
MitoCOX-ICUE1	Mitochondrial matrix	Amino acid 1-12 of subunit IV of human cytochrome oxidase *c* (COX) fused to the N-terminus		
4mtH30	Mitochondria	Repetitive (four copies) targeting sequences from subunit VIII of the human cytochrome oxidase (COX) fused to the N terminus	n.a.	(70)
Pm-AKAR3	Plasma membrane	Plasma membrane sequence KKKKKSKTKCVIM fused to the C-terminus	CMV	(65)
AKAR3-NES	Cytoplasm	NES Sequence LPPLERLTL sequence fused to the C-terminus		
AKAR3-NLS	Nucleus	NLS sequence PKKKRKVEDA fused to the C-terminus		
4mt-Epac-SH187	Mitochondria	Targeting sequence 4mt, encoding four copies of the signal sequence from subunit VIII of human cytochrome *C* oxidase, fused to the N-terminus	CMV	(72)

DAKAP-AKAR3	Mitochondria	MAIQLRSLFPLALPGMLALLGWWWFFSRKK from DAKAP-1a fused to the N-terminus	CMV	(24)
OMM-EpacH90	Outer mitochondrial membrane	Peptide yTOM70 introduced at the N-Terminus of the different sensors	n.a.	(73)
OMM-AKAR3	Outer mitochondrial membrane			
OMM-AKAR4	Outer mitochondrial membrane			
Mito-EpacH90	Mitochondria	Repetitive (four copies) targeting sequence from subunit VIII of the cytochrome oxidase (COX) (from mito-D3cpv) introduced into the N terminus	n.a.	
Mito-AKAR3	Mitochondria			
Mito-AKAR4	Mitochondria			
ER-bPAC-nLuc	Endoplasmic reticulum	18-amino acid BiP signal sequence + AKDEL fused to the N-terminus	CMV	(74)
bPAC–nLuc-CAAX	Plasma membrane	Targeting sequence of KRas4B-CVIM		
NLS–bPAC–nLuc	Nucleus	NLS sequence PKKKRKVEDA	CMV	(74)
NES–bPAC–nLuc	Cytoplasm	NES sequence LQLPPLERLTL		
MYR–bPAC–nLuc	Plasma membrane	Amino acids 1-17 of the Yes protein fused to the N-terminus		
pmEpac1	Plasma membrane	N-terminal 10 amino acid peptide MGSINSKRKD of Lyn kinase fused to the N-terminus	Alpha-MHC (alpha myosin heavy chain)	(79)
pm-EPAC2	Plasma membrane	`SH4' motif (MGCINSKRKD) of Lyn kinase	n.a.	(80)
Epac1-PLN	Sarcoplasmic reticulum	PLN (aa 2-52) fused to the C-terminus	n.a.	(77)
PLM-Epac1	SERCA2a microdomain	Full-length canine PLM without a stop codon fused to the N-terminus via a flexible linker (KRSRAQASNSAVDGTPVATG)	n.a.	(78)
SR-AKAR3	Sarcoplasmic reticulum	PQQARQKLQNLFINFCLILICLLLICIIVMLL of PLN fused to the N-terminus	CMV	(81)
EPAC-JNC	Proximity to RyR2	Full-length mouse JNC and a flexible helical linker (GSMPLVDFFC) fused to the C-terminus	Alpha-MHC	(82)
Prm1-bPAC	post-meiotic spermatids	-	Prm1	(50)
Prm1-LAPD	post-meiotic spermatids	-	Prm1	(51)
Prm1-mlCNBD-FRET	post-meiotic spermatids	-	Prm1	(85)
SSTR3-mlCNBD-FRET	Primary cilia	SSTR3 fused to the N-terminus	n.a.	

5-HT6-mcherry-cADDis	Primary cilia	5-HT6 receptor fused to the N-terminus	n.a.	(46)
Arl13b-H188 and Arl13b-H187	Primary cilia	Arl13b inserted into the N-terminus of Epac-H187 and Epac-H188	n.a.	(86)
5-HT6-EpacH187	Primary cilia	5-HT6 receptor inserted into the N-terminus of Epac-H187		

References

1. Gerits N, Kostenko S, Shiryaev A, Johannessen M, & Moens U (2008) Relations between the mitogen-activated protein kinase and the cAMP-dependent protein kinase pathways: comradeship and hostility. *Cell. Signal.* 20(9):1592-1607.
2. Sassone-Corsi P (2012) The cyclic AMP pathway. *Cold. Spring. Harb. Perspect. Biol.* 4(12).
3. Cooper DM (2003) Regulation and organization of adenylyl cyclases and cAMP. *Biochem. J.* 375(Pt 3):517-529.
4. Beavo JA & Brunton LL (2002) Cyclic nucleotide research -- still expanding after half a century. *Nat. Rev. Mol. Cell. Biol.* 3(9):710-718.
5. Lefkimmiatis K & Zaccolo M (2014) cAMP signaling in subcellular compartments. *Pharmacol. Ther.* 143(3):295-304.
6. Deisseroth K (2011) Optogenetics. *Nat. Methods.* 8(1):26-29.
7. Möglich A & Moffat K (2010) Engineered photoreceptors as novel optogenetic tools. *Photochem. Photobiol. Sci.* 9(10):1286-1300.
8. Kottke T, Xie A, Larsen DS, & Hoff WD (2018) Photoreceptors Take Charge: Emerging Principles for Light Sensing. *Annu. Rev. Biophys.*
9. Möglich A, Yang X, Ayers RA, & Moffat K (2010) Structure and function of plant photoreceptors. *Annu. Rev. Plant. Biol.* 61:21-47.
10. Ziegler T & Möglich A (2015) Photoreceptor engineering. *Front. Mol. Biosci.* 2:30.
11. Ryu MH, Moskvin OV, Siltberg-Liberles J, & Gomelsky M (2010) Natural and engineered photoactivated nucleotidyl cyclases for optogenetic applications. *J. Biol. Chem.* 285(53):41501-41508.
12. Stierl M*, et al.* (2011) Light modulation of cellular cAMP by a small bacterial photoactivated adenylyl cyclase, bPAC, of the soil bacterium Beggiatoa. *J. Biol. Chem.* 286(2):1181-1188.
13. Blain-Hartung M*, et al.* (2018) Cyanobacteriochrome-based photoswitchable adenylyl cyclases (cPACs) for broad spectrum light regulation of cAMP levels in cells. *J. Biol. Chem.* 293(22):8473-8483.
14. Ryu MH*, et al.* (2014) Engineering adenylate cyclases regulated by near-infrared window light. *Proc. Natl. Acad. Sci. USA.* 111(28):10167-10172.
15. Etzl S, Lindner R, Nelson MD, & Winkler A (2018) Structure-guided design and functional characterization of an artificial red light-regulated guanylate/adenylate cyclase for optogenetic applications. *J. Biol. Chem.* 293(23):9078-9089.
16. Rauch A, Leipelt M, Russwurm M, & Steegborn C (2008) Crystal structure of the guanylyl cyclase Cya2. *Proc. Natl. Acad. Sci. USA* 105(41):15720-15725.
17. Stüven B*, et al.* (2019) Characterization and engineering of photoactivated adenylyl cyclases. *Biol. Chem.* 400(3):429-441.

18. Scheib U*, et al.* (2018) Rhodopsin-cyclases for photocontrol of cGMP/cAMP and 2.3 A structure of the adenylyl cyclase domain. *Nat. Commun.* 9(1):2046.
19. Trieu MM*, et al.* (2017) Expression, purification, and spectral tuning of RhoGC, a retinylidene/guanylyl cyclase fusion protein and optogenetics tool from the aquatic fungus Blastocladiella emersonii. *J. Biol. Chem.* 292(25):10379-10389.
20. Tian Y, Gao S, Yang S, & Nagel G (2018) A novel rhodopsin phosphodiesterase from Salpingoeca rosetta shows light-enhanced substrate affinity. *Biochem. J.* 475(6):1121-1128.
21. Yoshida K, Tsunoda SP, Brown LS, & Kandori H (2017) A unique choanoflagellate enzyme rhodopsin exhibits light-dependent cyclic nucleotide phosphodiesterase activity. *J. Biol. Chem.* 292(18):7531-7541.
22. Lamarche LB*, et al.* (2017) Purification and Characterization of RhoPDE, a Retinylidene/Phosphodiesterase Fusion Protein and Potential Optogenetic Tool from the Choanoflagellate Salpingoeca rosetta. *Biochemistry* 56(43):5812-5822.
23. Gasser C*, et al.* (2014) Engineering of a red-light-activated human cAMP/cGMP-specific phosphodiesterase. *Proc. Natl. Acad. Sci. USA.* 111(24):8803-8808.
24. Allen MD & Zhang J (2006) Subcellular dynamics of protein kinase A activity visualized by FRET-based reporters. *Biochem. Biophys. Res. Commun.* 348(2):716-721.
25. Depry C, Allen MD, & Zhang J (2011) Visualization of PKA activity in plasma membrane microdomains. *Mol. Biosyst.* 7(1):52-58.
26. Zhang J, Hupfeld CJ, Taylor SS, Olefsky JM, & Tsien RY (2005) Insulin disrupts beta-adrenergic signalling to protein kinase A in adipocytes. *Nature.* 437(7058):569-573.
27. Zhang J, Ma Y, Taylor SS, & Tsien RY (2001) Genetically encoded reporters of protein kinase A activity reveal impact of substrate tethering. *Proc. Natl. Acad. Sci. USA.* 98(26):14997-15002.
28. Förster T (1946) Energiewanderung und Fluoreszenz. *Naturwissenschaften* 33(6):166-175.
29. Zaccolo M*, et al.* (2000) A genetically encoded, fluorescent indicator for cyclic AMP in living cells. *Nat. Cell. Biol.* 2(1):25-29.
30. Schleicher K & Zaccolo M (2018) Using cAMP Sensors to Study Cardiac Nanodomains. *J. Cardiovasc. Dev. Dis.* 5(1).
31. Zaccolo M & Pozzan T (2002) Discrete microdomains with high concentration of cAMP in stimulated rat neonatal cardiac myocytes. *Science.* 295(5560):1711-1715.
32. Hill SJ, Williams C, & May LT (2010) Insights into GPCR pharmacology from the measurement of changes in intracellular cyclic AMP; advantages and pitfalls of differing methodologies. *Br. J. Pharmacol.* 161(6):1266-1275.
33. Sprenger JU & Nikolaev VO (2013) Biophysical techniques for detection of cAMP and cGMP in living cells. *Int. J. Mol. Sci.* 14(4):8025-8046.

34. Willoughby D & Cooper DM (2008) Live-cell imaging of cAMP dynamics. *Nat. Methods.* 5(1):29-36.
35. Börner S*, et al.* (2011) FRET measurements of intracellular cAMP concentrations and cAMP analog permeability in intact cells. *Nat. Protoc.* 6(4):427-438.
36. Correa AC & Schultz C (2009) *Chapter 6 Small molecule-based FRET probes* (Elsevier B.V.).
37. Woehler A, Wlodarczyk J, & Neher E (2010) Signal/noise analysis of FRET-based sensors. *Biophys. J.* 99(7):2344-2354.
38. Bajar BT, Wang ES, Zhang S, Lin MZ, & Chu J (2016) A Guide to Fluorescent Protein FRET Pairs. *Sensors (Basel, Switzerland)* 16(9).
39. Surdo NC*, et al.* (2017) FRET biosensor uncovers cAMP nano-domains at beta-adrenergic targets that dictate precise tuning of cardiac contractility. *Nat. Commun.* 8:15031.
40. DiPilato LM & Zhang J (2009) The role of membrane microdomains in shaping beta2-adrenergic receptor-mediated cAMP dynamics. *Mol. Biosyst.* 5(8):832-837.
41. Klarenbeek J, Goedhart J, van Batenburg A, Groenewald D, & Jalink K (2015) Fourth-generation epac-based FRET sensors for cAMP feature exceptional brightness, photostability and dynamic range: characterization of dedicated sensors for FLIM, for ratiometry and with high affinity. *PLoS. One.* 10(4):e0122513.
42. Norris RP*, et al.* (2009) Cyclic GMP from the surrounding somatic cells regulates cyclic AMP and meiosis in the mouse oocyte. *Development (Cambridge, England)* 136(11):1869-1878.
43. Ohta Y*, et al.* (2016) Nontrivial Effect of the Color-Exchange of a Donor/Acceptor Pair in the Engineering of Forster Resonance Energy Transfer (FRET)-Based Indicators. *ACS. Chem. Biol.* 11(7):1816-1822.
44. Mo GC*, et al.* (2017) Genetically encoded biosensors for visualizing live-cell biochemical activity at super-resolution. *Nat. Methods.* 14(4):427-434.
45. Baird GS, Zacharias DA, & Tsien RY (1999) Circular permutation and receptor insertion within green fluorescent proteins. *Proc. Natl. Acad. Sci. USA.* 96(20):11241-11246.
46. Moore BS*, et al.* (2016) Cilia have high cAMP levels that are inhibited by Sonic Hedgehog-regulated calcium dynamics. *Proc. Natl. Acad. Sci. USA* 113(46):13069-13074.
47. Ohta Y, Furuta T, Nagai T, & Horikawa K (2018) Red fluorescent cAMP indicator with increased affinity and expanded dynamic range. *Sci. Rep.* 8(1):1866.
48. Ettinger A & Wittmann T (2014) Fluorescence live cell imaging. *Methods. Cell. Biol.* 123:77-94.
49. Wachten S, Schlenstedt J, Gauss R, & Baumann A (2006) Molecular identification and functional characterization of an adenylyl cyclase from the honeybee. *Journal of neurochemistry* 96(6):1580-1590.
50. Jansen V*, et al.* (2015) Controlling fertilization and cAMP signaling in sperm by optogenetics. *eLife* 4.

51. Raju DN, *et al.* (2019) Cyclic Nucleotide-Specific Optogenetics Highlights Compartmentalization of the Sperm Flagellum into cAMP Microdomains. *Cells.* 8(7).
52. Stabel R, *et al.* (2019) Revisiting and Redesigning Light-Activated Cyclic-Mononucleotide Phosphodiesterases. *J. Mol. Biol.* 431(17):3029-3045.
53. Wunder F, Gnoth MJ, Geerts A, & Barufe D (2009) A novel PDE2A reporter cell line: characterization of the cellular activity of PDE inhibitors. *Mol. Pharm.* 6(1):326-336.
54. Corbin JD, Sugden PH, Lincoln TM, & Keely SL (1977) Compartmentalization of adenosine 3':5'-monophosphate and adenosine 3':5'-monophosphate-dependent protein kinase in heart tissue. *The Journal of biological chemistry* 252(11):3854-3861.
55. Nikolaev VO, Bunemann M, Hein L, Hannawacker A, & Lohse MJ (2004) Novel single chain cAMP sensors for receptor-induced signal propagation. *J. Biol. Chem.* 279(36):37215-37218.
56. Perera RK & Nikolaev VO (2013) Compartmentation of cAMP signalling in cardiomyocytes in health and disease. *Acta. Physiol. (Oxf)* 207(4):650-662.
57. Lingwood D & Simons K (2010) Lipid rafts as a membrane-organizing principle. *Science* 327(5961):46-50.
58. Agarwal SR, *et al.* (2014) Role of membrane microdomains in compartmentation of cAMP signaling. *PLoS. One.* 9(4):e95835.
59. Koschinski A & Zaccolo M (2017) Activation of PKA in cell requires higher concentration of cAMP than in vitro: implications for compartmentalization of cAMP signalling. *Sci. Rep.* 7(1):14090.
60. Iancu RV, Jones SW, & Harvey RD (2007) Compartmentation of cAMP signaling in cardiac myocytes: a computational study. *Biophys. J.* 92(9):3317-3331.
61. Beck S, *et al.* (2018) Synthetic Light-Activated Ion Channels for Optogenetic Activation and Inhibition. *Front. Neurosci.* 12:643.
62. Bernal Sierra YA, *et al.* (2018) Potassium channel-based optogenetic silencing. *Nat. Commun.* 9(1):4611.
63. Zippin JH, *et al.* (2004) Bicarbonate-responsive "soluble" adenylyl cyclase defines a nuclear cAMP microdomain. *The Journal of Cell Biology* 164(4):527-534.
64. DiPilato LM, Cheng X, & Zhang J (2004) Fluorescent indicators of cAMP and Epac activation reveal differential dynamics of cAMP signaling within discrete subcellular compartments. *Proc. Natl. Acad. Sci. USA.* 101(47):16513-16518.
65. Sample V, *et al.* (2012) Regulation of nuclear PKA revealed by spatiotemporal manipulation of cyclic AMP. *Nat. Chem. Biol.* 8(4):375-382.
66. Valsecchi F, Ramos-Espiritu LS, Buck J, Levin LR, & Manfredi G (2013) cAMP and mitochondria. *Physiology (Bethesda)* 28(3):199-209.
67. Acin-Perez R, Gatti DL, Bai Y, & Manfredi G (2011) Protein phosphorylation and prevention of cytochrome oxidase inhibition by ATP:

coupled mechanisms of energy metabolism regulation. *Cell Metab.* 13(6):712-719.
68. Acin-Perez R*, et al.* (2011) A phosphodiesterase 2A isoform localized to mitochondria regulates respiration. *J. Biol. Chem.* 286(35):30423-30432.
69. Acin-Perez R*, et al.* (2009) Cyclic AMP produced inside mitochondria regulates oxidative phosphorylation. *Cell Metab.* 9(3):265-276.
70. Di Benedetto G, Scalzotto E, Mongillo M, & Pozzan T (2013) Mitochondrial Ca(2)(+) uptake induces cyclic AMP generation in the matrix and modulates organelle ATP levels. *Cell Metab.* 17(6):965-975.
71. Ponsioen B*, et al.* (2004) Detecting cAMP-induced Epac activation by fluorescence resonance energy transfer: Epac as a novel cAMP indicator. *EMBO. Rep.* 5(12):1176-1180.
72. Wang Z*, et al.* (2016) A cardiac mitochondrial cAMP signaling pathway regulates calcium accumulation, permeability transition and cell death. *Cell. Death. Dis.* 7:e2198.
73. Lefkimmiatis K, Leronni D, & Hofer AM (2013) The inner and outer compartments of mitochondria are sites of distinct cAMP/PKA signaling dynamics. *J. Cell Biol.* 202(3):453-462.
74. Naim N*, et al.* (2019) Luminescence-activated nucleotide cyclase regulates spatial and temporal cAMP synthesis. *J. Biol. Chem.* 294(4):1095-1103.
75. Rost BR, Schneider-Warme F, Schmitz D, & Hegemann P (2017) Optogenetic Tools for Subcellular Applications in Neuroscience. *Neuron.* 96(3):572-603.
76. Ghigo A & Mika D (2019) cAMP/PKA signaling compartmentalization in cardiomyocytes: Lessons from FRET-based biosensors. *J. Mol. Cell. Cardiol.* 131:112-121.
77. Sprenger JU*, et al.* (2015) In vivo model with targeted cAMP biosensor reveals changes in receptor-microdomain communication in cardiac disease. *Nat. Commun.* 6:6965.
78. Bastug-Özel Z*, et al.* (2019) Heart failure leads to altered beta2-adrenoceptor/cyclic adenosine monophosphate dynamics in the sarcolemmal phospholemman/Na,K ATPase microdomain. *Cardiovasc. Res.* 115(3):546-555.
79. Perera RK*, et al.* (2015) Microdomain switch of cGMP-regulated phosphodiesterases leads to ANP-induced augmentation of beta-adrenoceptor-stimulated contractility in early cardiac hypertrophy. *Circ. Res.* 116(8):1304-1311.
80. Wachten S*, et al.* (2010) Distinct pools of cAMP centre on different isoforms of adenylyl cyclase in pituitary-derived GH3B6 cells. *J. Cell Sci.* 123(Pt 1):95-106.
81. Liu S, Zhang J, & Xiang YK (2011) FRET-based direct detection of dynamic protein kinase A activity on the sarcoplasmic reticulum in cardiomyocytes. *Biochem. Biophys. Res. Commun.* 404(2):581-586.
82. Berisha F*, et al.* (2019) Direct monitoring of cAMP at the cardiac ryanodine receptor using a novel targeted fluorescence biosensor mouse. *bioRxiv*:623934.

83. Balbach M, Beckert V, Hansen JN, & Wachten D (2018) Shedding light on the role of cAMP in mammalian sperm physiology. *Mol. Cell. Endocrinol.* 468:111-120.
84. Johnson JL & Leroux MR (2010) cAMP and cGMP signaling: sensory systems with prokaryotic roots adopted by eukaryotic cilia. *Trends Cell Biol.* 20(8):435-444.
85. Mukherjee S*, et al.* (2016) A novel biosensor to study cAMP dynamics in cilia and flagella. *eLife* 5.
86. Jiang JY, Falcone JL, Curci S, & Hofer AM (2019) Direct visualization of cAMP signaling in primary cilia reveals up-regulation of ciliary GPCR activity following Hedgehog activation. *Proc. Natl. Acad. Sci. USA* 116(24):12066-12071.
87. Sherpa RT*, et al.* (2019) Sensory primary cilium is a responsive cAMP microdomain in renal epithelia. *Sci. Rep.* 9(1):6523.
88. O'Banion CP*, et al.* (2018) Design and Profiling of a Subcellular Targeted Optogenetic cAMP-Dependent Protein Kinase. *Cell. Chem. Biol.* 25(1):100-109.e108.
89. Ohki M*, et al.* (2016) Structural insight into photoactivation of an adenylate cyclase from a photosynthetic cyanobacterium. *Proc. Natl. Acad. Sci. USA.* 113(24):6659-6664.
90. Iseki M*, et al.* (2002) A blue-light-activated adenylyl cyclase mediates photoavoidance in Euglena gracilis. *Nature* 415(6875):1047-1051.
91. Penzkofer A, Stierl M, Hegemann P, & Kateriya S (2011) Photo-dynamics of the BLUF domain containing soluble adenylate cyclase (nPAC) from the amoeboflagellate Naegleria gruberi NEG-M strain. *Chem. Phys.* 387(1):25-38.
92. Penzkofer A*, et al.* (2013) Photo-dynamics and thermal behavior of the BLUF domain containing adenylate cyclase NgPAC2 from the amoeboflagellate Naegleria gruberi NEG-M strain. *Chem. Phys.* 412:96-108.
93. Penzkofer A*, et al.* (2014) Photo-dynamics of BLUF domain containing adenylyl cyclase NgPAC3 from the amoeboflagellate Naegleria gruberi NEG-M strain. *J. Photochem. Photobiol. C.* 287:19-29.
94. Raffelberg S*, et al.* (2013) A LOV-domain-mediated blue-light-activated adenylate (adenylyl) cyclase from the cyanobacterium Microcoleus chthonoplastes PCC 7420. *Biochem. J.* 455(3):359-365.
95. Nikolaev VO, Bünemann M, Schmitteckert E, Lohse MJ, & Engelhardt S (2006) Cyclic AMP imaging in adult cardiac myocytes reveals far-reaching beta1-adrenergic but locally confined beta2-adrenergic receptor-mediated signaling. *Circ. Res.* 99(10):1084-1091.
96. Hackley CR, Mazzoni EO, & Blau J (2018) cAMPr: A single-wavelength fluorescent sensor for cyclic AMP. *Sci. Signal.* 11(520).
97. Harada K*, et al.* (2017) Red fluorescent protein-based cAMP indicator applicable to optogenetics and in vivo imaging. *Sci. Rep.* 7(1):7351.
98. Tewson PH, Martinka S, Shaner NC, Hughes TE, & Quinn AM (2016) New DAG and cAMP Sensors Optimized for Live-Cell Assays in Automated Laboratories. *J. Biomol. Screen.* 21(3):298-305.

99. Odaka H, Arai S, Inoue T, & Kitaguchi T (2014) Genetically-encoded yellow fluorescent cAMP indicator with an expanded dynamic range for dual-color imaging. *PLoS. One.* 9(6):e100252.
100. Kitaguchi T, Oya M, Wada Y, Tsuboi T, & Miyawaki A (2013) Extracellular calcium influx activates adenylate cyclase 1 and potentiates insulin secretion in MIN6 cells. *Biochem. J.* 450(2):365-373.